

# Compatibility analysis of 3D printer resin for biological applications

Shilpa Sivashankar<sup>1</sup> ✉, Sumeyra Agambayev<sup>1</sup>, Kholod Alamoudi<sup>2</sup>, Ulrich Buttner<sup>1</sup>, Niveen Khashab<sup>2</sup>, Khaled Nabil Salama<sup>1</sup>

<sup>1</sup>Computer, Electrical and Mathematical Science and Engineering Division (CEMSE), King Abdullah University of Science and Technology (KAUST), Thuwal 23955-6900, Saudi Arabia

<sup>2</sup>Smart Hybrid Materials Laboratory (SHMs), Advanced Membranes and Porous Materials Center, King Abdullah University of Science and Technology (KAUST), Thuwal 23955-6900, Saudi Arabia

✉ E-mail: Shilpa.sivashankar@kaust.edu.sa

Published in *Micro & Nano Letters*; Received on 17th August 2016; Accepted on 25th August 2016

The salient features of microfluidics such as reduced cost, handling small sample and reagent volumes and less time required to fabricate the devices has inspired the present work. The incompatibility of three-dimensional printer resins in their native form and the method to improve their compatibility to many biological processes via surface modification are reported. The compatibility of the material to build microfluidic devices was evaluated in three different ways: (i) determining if the ultraviolet (UV) cured resin inhibits the polymerase chain reaction (PCR), i.e. testing devices for PCR compatibility; (ii) observing agglutination complex formed on the surface of the UV cured resin when anti-C-reactive protein (CRP) antibodies and CRP proteins were allowed to agglutinate; and (iii) by culturing human embryonic kidney cell line cells and testing for its attachment and viability. It is shown that only a few among four in its native form could be used for fabrication of microchannels and that had the least effect on biological molecules that could be used for PCR and protein interactions and cells, whereas the others were used after treating the surface. Importance in building lab-on-chip/micrototal analysis systems and organ-on-chip devices is found.

**1. Introduction:** In the past three decades, microfluidics has emerged from a one-functional device to multi-functional analytical devices with wide ranges of applications biological applications to, proteomics and metabolomics, in drug discovery [1], cell analysis, point-of-care (POC) devices [2, 3], genetic analysis [4, 5], organ-on-chip [6–9], and immunoassays [10, 11]. Though traditional laboratory equipment has been used for the above-mentioned assays, microfluidic devices to a greater extent have numerous merits over the macrosystems because it reduces sample volume, reduces reagent cost, is disposable and streamlines complex assay protocols [12]. These merits account for the development of laboratory-based POC diagnostic microfluidics systems and high-throughput analytical devices to be foreseen [13]. These minuscule devices' dimensions vary between millimetres and micrometres and perform task ranging from detecting airborne toxins to analysing spheroids/three-dimensional (3D) tissues, thus emphasising the requirement of biocompatible materials to investigate the studies. The need for biocompatible materials to fabricate the microfluidic device arises because they greatly enhance or improve methods for biomedical applications [14].

The most time-consuming and tedious techniques of obtaining microchannels are via photolithography and soft lithography [15] due to the involvement of numerous sequential steps that need to be followed during fabrication. Designs of microfluidic microchannels are usually limited to single depth planar geometries via lithography techniques. Though the masks used to create multilayered channels are expensive and tedious to produce, it is possible to create multilayered channels by a lithography process. With these effort put in, there is also the possibility of contamination of PDMS microchannels formed using lithographic moulds [16], and hence only skilled person succeeds in creating very precise multilayered channels. Microchannels are also fabricated using other techniques such as laser writing [17–19], dry etching [20], injection-moulding technique [21], embossing and imprinting technique [22], and the latest being foam folding method [23], but these

are again tedious and time-consuming [24]. Also, these processes need continuous monitoring when fabricating a device.

Researchers would choose to opt for a simple, easy, and quick fabrication process rather than time-consuming and tedious process as these processes need time to be well-trained [25]. The recent advances in 3D printing technologies are preferred and aid in the drastic reduction of time and skills required for fabricating a device favouring researchers. Recently, 3D printed microfluidics have contributed substantially regarding cost cutting to the fabrication of advanced lab-on-chip devices to biomedical field [26]. While traditional methods such as microelectro mechanical systems lithography, soft lithography [27], and 3D printed-paper-based microfluidics to assess agglutination on a chip [28] maybe expensive and require more time to fabricate a device unlike 3D printing technology [29, 30]. Microfluidics has gained importance with the introduction of 3D printing technologies to produce complex 3D structures without the hassle of a time-consuming process such as photolithography or soft lithography [31–35]. Though 3D printing has been developing rapidly, microfluidic developers avoid the adoption of 3D printing due to certain barriers on the resolution, throughput, and resin biocompatibility [36].

3D printers have many merits such as they are inexpensive, less time-consuming, and are automated; unlike photolithography they also have demerits. One of the demerits is that they are incompatible with most biological applications. Hence, we study the compatibility of the resin to few biological applications that involve the interaction with DNA, proteins, and cells. We performed polymerase chain reaction (PCR), cell viability assay, and agglutination to confirm the biocompatible issues. The PCR compatibility of silicon, silicon dioxide, polyethylene glycol diacrylate, and other surfaces have been studied [34, 37, 38]. Though 3D printer resins [39] have been tested before for cell application using phormidium and shown not to be biocompatible, we show PCR reactions, agglutination reactions, and cell studies can be performed using some of the resins tested.

**Table 1** Sequence used for amplification

Name	Sequence
16S rDNA <i>Escherichia coli</i>	5' GTGCCAGCAGCCGCGGTAATACGGA GGTGCAAGCGTTAATCGGAATTACTGGGCGTAAAGCG 3'
primer 1 27F	5' AGAGTTTGTATCMTGGCTCAG 3'
primer 2 1492R	5' TACGGYTACCTTGTACGACTT 3'

We developed a comparative study between the solid ultraviolet (UV) curable resin in native form and surface-modified resin for biological application such as PCR, immunoassay, and cell studies. A simple, relatively quick measurement study was designed that requires only a thermocycler to amplify the selected gene sequence. We assessed the inhibitory effect of four types of 3D printer resins for PCR and agglutination reactions as these are considered to be most frequently used enzymatic reactions in microfluidics. When assessed, we found that only certain type of resins can be utilised for these biological reactions in their native form. Therefore, the surface of the resin was treated to evaluate the biocompatibility of the resin. The incorporated surface modification techniques on all the four types of resin yielded in utilising the resins that for PCR/agglutination reactions and cell-related studies. The proposed study finds importance in assessing which kind of resin would benefit particular biological applications and building a biocompatible microfluidic device.

## 2. Materials and methods

**2.1. Samples:** Resins were purchased from FormLabs and Kudo with a definite composition for hardness, transparency, and elasticity, as there were the critical parameters required to build any microfluidic device. Resin's compatibility for various applications was evaluated by performing an immunoassay, PCR reactions, and culturing cells on the surface. The reaction mixtures and PCR components, and materials were purchased from Fisher scientific and Invitrogen. The thermocycler employed was from Applied Biosystems. Standard C-reactive protein (CRP) test kits (Arlington Scientific, Inc. (ASI), Arlington) and human CRP serum (Pronac) were utilised in all of the experiments. The kits consist of beads coated with anti-CRP antibodies, analyte, and azide buffer. All dilutions were made using this azide buffer.

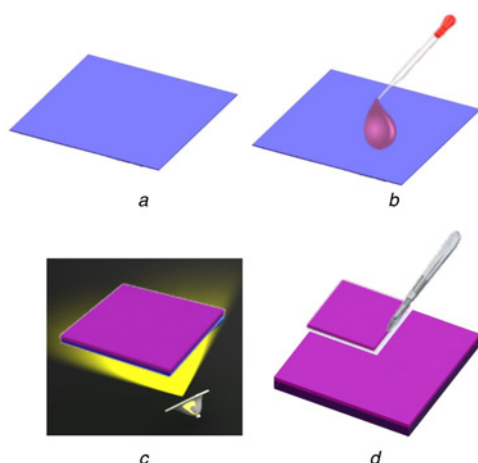


**Fig. 1** Fabrication procedure of resin for characterisation  
*a* Clean glass slide  
*b* Resin dispersed on glass  
*c* 3D printed to form a layer of 200 µm  
*d* Cut the resin using surgical knife

**2.2. Amplification sequence:** The sequence to be amplified was synthesised, and the following table represents the sequence of the target DNA and primers used for amplification. The 1500 bp DNA was utilised throughout the experiments (Table 1).

**2.3. Characterisation of fabricated resin:** Microfluidic channels are either designed using Windows Paint, PowerPoint, or Solid-Works software program for Windows 7 on a 64 bit computer operating system. Sliced templates are imported to the Kudo3D the Titan 1 printer as a PNG or Bitmap file as well. Kudo Titan 3D printer was used to solidify 200 µm thick resin by exposing the resin for 10 s. Different composition and material property of UV curable resins were characterised for biocompatibility. The images are imported to the printer using Kudo open source 3D printer software. A glass slide cleaned with alcohol of dimensions 25 × 25 mm was attached to the stage of the 3D printer as substrate. The tray of the 3D printer was filled with the particular resin to be tested. The printer exposes the image for 10 s, and the resin is cured when exposed to UV on the substrate. In this case, we used only one image to fabricate a layer of resin with an exposure of 10 s yielding a thickness of 200 µm. The fabrication procedure is detailed in Fig. 1. The fabricated resin, broken into small fragments of size <5 mm<sup>2</sup> using a surgical knife was utilised for all the experiments.

## 2.4. Surface modification

**2.4.1. BSA surface treatment:** Surface modification of the resin involved four major steps. First, on curing the resin for 10 s under UV, it was washed with IPA thoroughly and immersed in ethyl alcohol for 5 min. Second, it was treated with 1 M HCl for 2 min. Third, the resin was treated with 1 M NaOH for 2 min. Finally, these fragmented resins were dipped in 0.5 mg/ml BSA for 30 min. For cell culture, the incubation time for BSA was 4 h. This resulted in coating BSA to the entire surface of the resin. The resins were then immersed in water to remove any free BSA on the surface. Also, the surface modification opened new doors for testing the material compatibility for the targeted biological applications (PCR compatibility and agglutination assay). The detailed procedure of surface modifications is illustrated in Fig. 2.

**2.5. Procedure for PCR:** The fabricated, fragmented resin is mixed with target DNA, primer, and master mix and rocked on a rocker platform for 30 min. An illustration of the procedure for material incubation with the PCR components is explained in Fig. 3. Target DNA (16S rDNA) was diluted with DI water to 10 ng/µl.

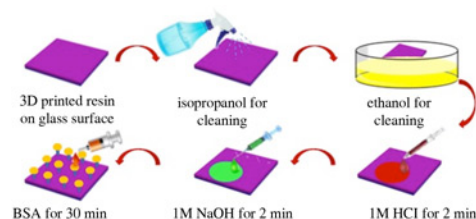
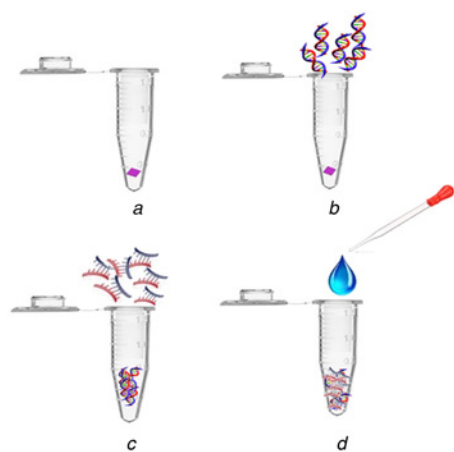


**Fig. 2** Modification procedure of the 3D printed resin



PCR conditions × 35 cycles	
temperature (°C)	time (sec)
96	60
96	10
56.5	5
60	420

**Fig. 3** Schematic illustration of PCR process

- a PCR tube with resin
- b Addition of 16S rDNA
- c Addition of primers
- d Addition of master mix

The 16S rDNA was mixed with a set of primers 27F, 1429R, and Invitrogen master mix. The total volume of the PCR mixture was maintained to 20  $\mu$ l by adding 8  $\mu$ l of 10 ng/ $\mu$ l of 16S rDNA, 1  $\mu$ l 27F, and 1  $\mu$ l 1429R along with 10  $\mu$ l master mix. About 35 cycles of PCR were performed with initial denaturation temperature starting at 96°C for 1 min, for the first cycle, and for the consecutive 34 cycles the same denaturation temperature was set to 10 s. The annealing and extension temperatures were set to 56.5°C for 5 s and 60°C for 7 min throughout the PCR run, respectively. However, for the final step, the extension temperature was set to 4°C forever. The whole PCR product and fragments were analysed by electrophoresis.

**2.6. Procedure for gel electrophoresis:** PCR amplified product was visualised by agarose gel electrophoresis technique. The amplified product was mixed with dye and loaded onto wells and allowed to run for 45 min acquiring the amplified that is visible by a UV detector. An illustration of the gel electrophoresis technique is detailed in Fig. 4. About 0.5 g of agarose was weighed and added to 50 ml of TAE buffer. Agarose was dissolved in TAE buffer on heating the mixture in the microwave for about 3 min. The liquefied mixture was poured onto the gel tray using a nine well comb, then placed in the right groove and allowed to settle for about 20 min. On cooling, the liquefied agarose turned into a solidified gel. The inserted comb was removed after solidification of the gel to form wells for loading the sample. The gel tray is filled with 300 ml TAE buffer. About 5  $\mu$ l of the amplified PCR product was mixed with 2  $\mu$ l of dye and added to the wells. Five samples were loaded into five different wells (one being control and the other four incubated with four types of resins), and the sixth well was loaded with DNA ladder for the reference. Sixth well was mixed with 2  $\mu$ l DNA ladder and 2  $\mu$ l dye as a reference

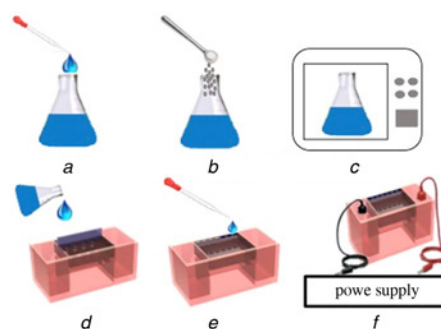


**Fig. 4** Schematic illustration of gel electrophoresis procedure

- a TAE buffer
- b Agarose added to TAE buffer
- c Microwave to dissolve agarose
- d Liquefied agarose added to gel tray
- e Sample added to wells
- f Connected to power supply and run the gel

of the amplified product moved through the porous gel. The results were compared with the control, where traditional PCR was performed using a commercially available PCR tube. The tray was connected to power source, and a voltage of 120 V was applied across the device. Electrophoresis was carried out for about 45 min. The processed gel was then viewed using a UV illuminator to acquire data about the displacement of the amplified product through the gel.

**2.7. Cell culture and viability assay:** Human embryonic kidney cell line (HEK) cells were cultured in DMEM media supplemented with 10% foetal bovine serum and 1% penicillin–streptomycin at 37°C in a 5% CO<sub>2</sub> humidified atmosphere. After cell detachment, the cell suspension was centrifuged, the pellet was collected, and cells were counted for further plating. HEK cells were seeded in 24-well plates at a density of  $5 \times 10^4$ /well. After 24 h, cells were seeded on four different types of native and modified material. The incubation of cells with test samples lasts for 24 h at 37°C. Phase contrast images were obtained to assess the growth of the cultured cells.

**3. Results and discussion:** In this Letter, we describe a surface modification method for four types of 3D printer resins to be compatible for PCR, agglutination reactions, and cell culture. These four resins were chosen because each of these resins belongs to different categories that would make it suitable for building microfluidic devices. Spot-elastic (Spot-E), spot-hard and tough (Spot-HT), FormLabs clear, and Venus have flexible, tough, compressible, and transparent nature, respectively. Spot-E being elastic in nature would be used to build flexible microfluidic devices for gas and liquid applications [40]. Spot-HT adopting HT feature could be used for building microfluidic pumps and valves that are in contact with the biological samples [41]. FormLabs clear that is compressible and transparent, but not flexible could find application in building microchannels that need to be sandwiched between two substrates for detection [13]. Venus clear that is transparent in appearance can be used for creating microchannels that involve biological samples in two-phase flow systems [42]. The proposed work focuses onto test for the compatibility of the resin to build a microfluidic device that inculcates protein, enzymatic (PCR), and cell interactions. Resins were fabricated in the form of thin films and analysis if protein and cell interaction on the surface were studied. While the resin was cut into small fragments and incubated with the sample for 30 min to observe possible

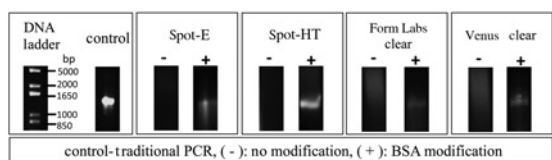


**Fig. 5** PCR

a Before modification  
b After modification

interference of the resins for PCR. The resins in their native form were incompatible with the tested biological applications calling in for surface treatment. We suppose that the molecules tend to attach to the surface of the walls that are in contact with the biomolecules such as in PDMS [43, 44]. To overcome this, we treated the surface using chemical solutions. We were certain that the surface of the resin interacted with the proteins and DNA molecules, and this inhibited the PCR and agglutination process in some of the resin types during a pilot study. Henceforth, the modification performed on the resin, coated the surface with BSA preventing the biomolecule attachment on the surface of the resin. Subsequent to the acid/base treatment, the channels were injected with DI water to clean the inner surface of the microchannels. This incorporation of surface treatment to the resin greatly enhanced experimental outcomes.

With the ionic treatment and coating of BSA on the surface, there was no free resin surface to bond with the biomolecule that was used. The resin was tested before and after surface modification of the surface and confirmed in triplicate experiments for each application. The results of PCR compatibility before modification (-) and after modification (+) are represented in Fig. 5 for each type of resin and compared with control and ladder for reference. The amplification of DNA is confirmed by the presence of bright bands as enumerated in Fig. 5. The bands are not very bright in Spot-E and FormLabs clear. One of the reasons for this behaviour might be due to the interaction of the resin with DNA molecules. The DNA molecules never travelled through any of the chosen resin in their native form. This maybe due to resin interacting with DNA strands, and hence not suitable for microfluidic applications, whereas the results after modification suggested that the observed bright band enabled the use of resin for PCR application. The trail observed with Spot-E is the possibility of resin and BSA interfering with the sample. The band was not very bright in FormLabs clear maybe due to interference resin components and BSA with the DNA molecules changing the concentration of the original sample. Therefore, we suggest 0.2 mg/ml of BSA be used for coating the surface and to reduce the trailing effect during PCR. Again this suggests that there is a partial interaction of the material, and hence may not be suitable for microfluidic devices. On the other hand, when treated, the results reveal the surface-modified resins, i.e. all four types of resins can be used for PCR, but Spot-HT and Venus are better options to choose for PCR compatible applications.

Protein inhibitory effect was verified via immunoassay technique. The test involved, the reaction between anti-CRP antibodies and CRP proteins resulting in clumps. The results of the immunoassay in native form are revealed in Fig. 6a. When an antibody interacts with a specific antigen, they form clumps and is called agglutination complex. The complexes appear within 10 s after an agglutinant and an agglutinate are in contact. The agglutination complex was not prominent in Spot-E, Spot-HT, and Venus clear when used in the native form. However, some small complexes were observed indicating that it might need more proteins to form a clump. It is worth noting that a clear agglutination clump similar to control were formed in FormLabs clear resin in native form, but with reduced concentration for the same amount of proteins interacted. This reduction in the concentration of the sample indicates that the resin would have absorbed the CRP into its pores. A clear agglutination trend was noted in Spot-E, Spot-HT,

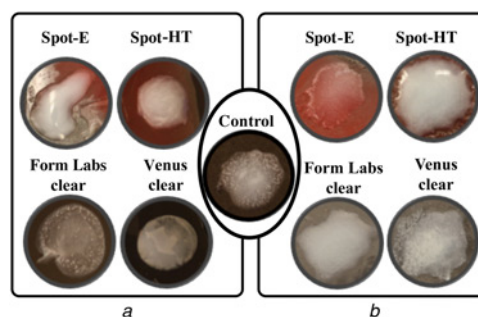


**Fig. 6** Agglutination

a Before modification  
b After modification

FormLabs clear, and Venus (after 10 s) resins after BSA modification in Fig. 6b implying that these were suitable for agglutination reaction. The agglutination process not being observed on the surfaces before modification maybe due to absorption of the protein on the resin inhibiting the agglutination process. This also implies that these resins could not be used for the process that involves protein interactions. However, after modification on the surface of the resin, we see that the agglutination is observed in all the four types of resin tested. Resins used for the experiments, before and after modification, and their compatibility with the protein interaction tested is tabulated in Table 2.

We also tested the resin biocompatibility by culturing HEK cells in native and BSA-modified surfaces. We printed thin films of the resins in a 24-well plate and modified the surface for cell culture. Two types of surface modification techniques were compared with the non-modified (native) resins. Phase contrast microscope (Nikon Ti-S, Japan) was used to obtain images to infer the results. We found the morphology of cells was not good showing the cells were unhealthy in non-modified and BSA-modified resins. Studies reveal the biocompatibility of the planar surface could be improved via surface modification of certain proteins and chemicals [45]. Therefore, we employed poly-L-lysine surface modification procedure for cell studies. The cured and cleaned substrates were treated with oxygen plasma for 3 min (Harrick Plasma-PDC 32G) and subsequently immersed in 10% APTES (v/v in water) (Sigma-Aldrich, Singapore) at 54°C for 120 min. The substrates were thoroughly washed in nuclease-free water and immersed in 0.01% of poly-L-lysine solution for 4 h. Finally, the substrates were prepared for cell culture by removing the solution, washing twice in nuclease-free water, and sterilising under UV light for 60 min.

The surface treated with poly-L-lysine had many viable cells and was found to be suitable for direct cell-seeding studies shown by phase contrast images in Fig. 7. Again, four types of resins were utilised for the present study due to their unique features. Each set of modification had a control that involved only BSA/poly-lysine modification (without resin) on the culture well. The morphology of cells for Spot-E appeared to be round, flat, and attached in poly-L-lysine treated when compared with non-modified and BSA-modified surface. While the cells were undergoing necrosis in the non-modified well which makes it look darker than the others. In Spot-HT, the cells appeared to be floating in the non-

**Table 2** Comparison of resin for protein compatibility before and after modification

Resin type	Before modification	After modification
Spot-E	-	compatible
Spot-HT	-	compatible
FormLabs clear	compatible	compatible
Venus clear	-	compatible

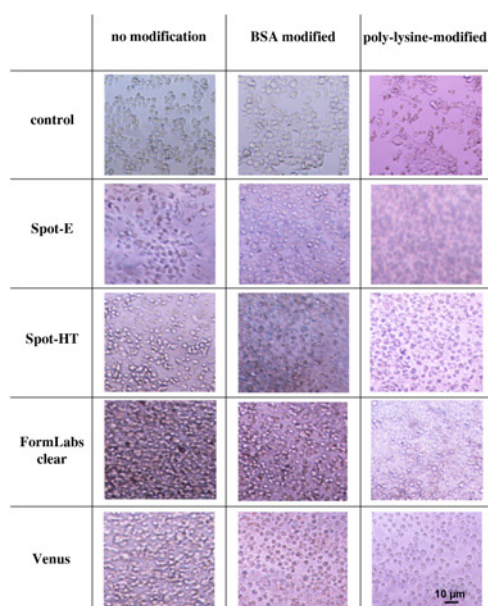


**Fig. 7** Morphology of cells via phase contrast images for native, BSA modified, and poly-l-lysine-modified surfaces

modified surface and the cells were slightly stretched in the BSA-modified surface. However, the cells were having round shape and better attachment in the poly-l-lysine-treated surfaces retained better morphology of the cells. Most of the cells from FormLabs clear resin for non-modified and BSA modified appeared to be floating while they still remain attached in poly-l-lysine-treated wells. This figure is not very clear because of the uneven thickness of the surface resulting due to the high viscosity of the resin. The cells in Venus clear for the non-modified group appears to be dead and hence floating. Whilst, the cells seem to be undergoing necrosis for BSA-treated group, and hence we observed dispersed particle like substances. However, the cells appeared to be rounded, but not completely attached to the poly-l-lysine-treated surface. These observations imply that these resins cannot be used for direct cell seeding and complete cellular studies while they can be surface treated with poly-l-lysine and avoid direct interference of resin components with the cells. Though poly-l-lysine is better than BSA treated and native forms of resins, we suggest that cells be seeded for short incubation time (<12 h) or be encapsulated within hydrogels [46] to completely avoid the chemical interaction of the photopolymer resins for organ-on-chip and tissue engineering applications.

**4. Conclusion:** To conclude, we investigated the interaction of the 3D printer resin for biological applications such as PCR, agglutination, and cell culture. Only a few resins in their native form can be used to build microfluidic devices. We, therefore, modified the surface that is in contact with the biomolecules. After the surface modification, all the four types of resins tested were found to be compatible with a variety of applications demonstrated. For short incubation (<12 h) cell culture studies, we suggest that poly-l-lysine be employed over the readily available BSA modification due to the better viability of the cultured cells. This Letter aids in building in vitro microfluidic devices that would be applicable for specific biological applications. Finally, we propose that this modification to the inner surface of the microchannels that are 3D printed leads to the development of cost-effective, disposable microfluidics devices with accelerated fabrication.

## 5 References

[1] Dittrich P.S., Manz A.: 'Lab-on-a-chip: microfluidics in drug discovery', *Nat. Rev. Drug Discov.*, 2006, **5**, (3), pp. 210–218

[2] Perez-Gonzalez V.H., Gallo-Villanueva R.C., Camacho-Leon S., *ET AL.*: 'Emerging microfluidic devices for cancer cells/biomarkers manipulation and detection', *IET Nanobiotechnol.*, 2016, doi:10.1049/iet-nbt.2015.0060

[3] Zheng Y., Sun Y.: 'Microfluidic devices for mechanical characterisation of single cells in suspension', *IET Micro Nano Lett.*, 2011, **6**, (5), pp. 327–331

[4] Sapsanis C., Sivashankar S., Omran H., *ET AL.*: 'Capacitive immunosensor for C-reactive protein quantification'. Proc. IEEE 58th Int. Midwest Symp. on Circuits and Systems (MWSCAS), Fort Collins, CO, 2–5 August 2015, p. 2015, pp. 1–4

[5] Liu P., Mathies R.A.: 'Integrated microfluidic systems for high-performance genetic analysis', *Trends Biotechnol.*, 2009, **27**, (10), pp. 572–581

[6] Kimura H., Yamamoto T., Sakai H., *ET AL.*: 'An integrated microfluidic system for long-term perfusion culture and on-line monitoring of intestinal tissue models', *Lab Chip*, 2008, **8**, (5), pp. 741–746

[7] Huh D., Matthews B.D., Mammoto A., *ET AL.*: 'Reconstituting organ-level lung functions on a chip', *Science*, 2010, **328**, (5986), pp. 1662–1668

[8] Tsai M., Kita A., Leach J., *ET AL.*: 'In vitro modeling of the microvascular occlusion and thrombosis that occur in hematologic diseases using microfluidic technology', *J. Clin. Invest.*, 2012, **122**, (1), pp. 408–418

[9] Huh D., Hamilton G.A., Ingber D.E.: 'From 3D cell culture to organs-on-chips', *Trends Cell Biol.*, 2011, **21**, (12), pp. 745–754

[10] Dishinger J.F., Kennedy R.T.: 'Serial immunoassays in parallel on a microfluidic chip for monitoring hormone secretion from living cells', *Anal. Chem.*, 2007, **79**, (3), pp. 947–954

[11] Mashraei Y., Sivashankar S., Buttner U., *ET AL.*: 'Integration of fractal biosensor in a digital microfluidic platform'. Proc. IEEE Sensors, 2015, Busan, South Korea, 1–4 November 2015, p. 2015

[12] Islam M., Natu R., Martinez-Duarte R.: 'A study on the limits and advantages of using a desktop cutter plotter to fabricate microfluidic networks', *Microfluidics Nanofluidics*, 2015, **19**, (4), pp. 973–985

[13] Sivashankar S., Sapsanis C., Buttner U., *ET AL.*: 'Flexible low-cost cardiovascular risk marker biosensor for point-of-care applications', *Electron. Lett.*, 2015, **51**, (22), pp. 1746–1747

[14] Faustino V., Catarino S.O., Lima R., *ET AL.*: 'Biomedical microfluidic devices by using low-cost fabrication techniques: a review', *J. Biomech.*, 2015, <http://dx.doi.org/10.1016/j.jbiomech.2015.11.031>

[15] Persano L., Camposo A., Pisignano D.: 'Integrated bottom-up and top-down soft lithographies and microfabrication approaches to multifunctional polymers', *J. Mater. Chem. C*, 2013, **1**, (46), pp. 7663–7680

[16] Bubendorfer A.J., Ingham B., Kennedy J.V., *ET AL.*: 'Contamination of PDMS microchannels by lithographic molds', *Lab Chip*, 2013, **13**, (22), pp. 4312–4316

[17] Zhang X., Huang D., Tang W., *ET AL.*: 'A low cost and quasi-commercial polymer film chip for high-throughput inertial cell isolation', *RSC Adv.*, 2016, **6**, (12), pp. 9734–9742

[18] Chung C.-K., Long H.P., Lai C.C.: 'Microfluidic chip using foil-assisted CO<sub>2</sub> laser ablation for suspended particle separation', *IET Micro Nano Lett.*, 2015, **10**, (10), pp. 500–503

[19] Sivashankar S., Agambayev S., Mashraei Y., *ET AL.*: 'A 'twisted' microfluidic mixer suitable for a wide range of flow rate applications', *Biomechanics*, 2016, **10**, (3), p. 034120

[20] Esashi M., Takinami M., Wakabayashi Y., *ET AL.*: 'High-rate directional deep dry etching for bulk silicon micromachining', *J. Micromech. Microeng.*, 1995, **5**, (1), p. 5

[21] Martynova L., Locascio L.E., Gaitan M., *ET AL.*: 'Fabrication of plastic microfluid channels by imprinting methods', *Anal. Chem.*, 1997, **69**, (23), pp. 4783–4789

[22] Klank H., Kutter J.P., Geschke O.: 'CO<sub>2</sub>-laser micromachining and back-end processing for rapid production of PMMA-based microfluidic systems', *Lab Chip*, 2002, **2**, (4), pp. 242–246

[23] He Y., Xiao X., Wu Y., *ET AL.*: 'A facile and low-cost micro fabrication material: flash foam', *Sci. Rep.*, 2015, **5**, p. 13522

[24] Lee M.P., Cooper G.J.T., Hinkley T., *ET AL.*: 'Development of a 3D printer using scanning projection stereolithography', *Sci. Rep.*, 2015, **5**, p. 9875

[25] Whitesides G.M.: 'Cool, or simple and cheap? Why not both?', *Lab Chip*, 2013, **13**, (1), pp. 11–13

[26] Ho C.M.B., Ng S.H., Li K.H.H., *ET AL.*: '3D printed microfluidics for biological applications', *Lab Chip*, 2015, **15**, (18), pp. 3627–3637

[27] He Y., Wu W.B., Fu J.Z.: 'Rapid fabrication of paper-based microfluidic analytical devices with desktop stereolithography 3D printer', *RSC Adv.*, 2015, **5**, (4), pp. 2694–2701

- [28] Sivashankar S., Castro D., Foulds I.G.: 'Real-time agglutination within a microdroplet in a three phase fluidic well for detection of bio-markers'. Proc. MicroTAS 2014, San Antonio, TX, 2014, pp. 1–3
- [29] Lee K.G., Park K.J., Seok S., *ET AL.*: '3D printed modules for integrated microfluidic devices', *RSC Adv.*, 2014, **4**, (62), pp. 32876–32880
- [30] Rogers C.I., Qaderi K., Woolley A.T., *ET AL.*: '3D printed microfluidic devices with integrated valves', *Biomicrofluidics*, 2015, **9**, (1), p. 016501
- [31] Chan H.N., Chen Y., Shu Y., *ET AL.*: 'Direct, one-step molding of 3D-printed structures for convenient fabrication of truly 3D PDMS microfluidic chips', *Microfluidics Nanofluidics*, 2015, **19**, (1), pp. 9–18
- [32] Buttner U., Sivashankar S., Agambayev S., *ET AL.*: 'Flash  $\mu$ -fluidics: a rapid prototyping method for fabricating microfluidic devices', *RSC Adv.*, 2016, **6**, (78), pp. 74822–74832
- [33] Reza A., Stephanie K., Alexander H., *ET AL.*: '3D-printed microfluidic devices', *Biofabrication*, 2016, **8**, (2), p. 022001
- [34] Sivashankar S., Agambayev S., Buttner U., *ET AL.*: 'Characterization of solid UV curable 3D printer resins for biological applications'. Proc. IEEE Nano Electro Mechanical Systems (NEMS) 2016, Matsushima, Japan, 2016, pp. 1–4
- [35] Comina G., Suska A., Filippini D.: 'Low cost lab-on-a-chip prototyping with a consumer grade 3D printer', *Lab Chip*, 2014, **14**, (16), pp. 2978–2982
- [36] Bhattacharjee N., Urrios A., Kang S., *ET AL.*: 'The upcoming 3D-printing revolution in microfluidics', *Lab Chip*, 2016, **16**, (10), pp. 1720–1742
- [37] Kodzius R., Xiao K., Wu J., *ET AL.*: 'Inhibitory effect of common microfluidic materials on PCR outcome', *Sens. Actuators B. Chem.*, 2012, **161**, (1), pp. 349–358
- [38] Castro D., Ingram P., Kodzius R., *ET AL.*: 'Characterization of solid UV cross-linked PEGDA for biological applications'. Proc. IEEE 26th Int. Conf. on Micro Electro Mechanical Systems (MEMS), 20–24 January 2013, 2013, pp. 1–4
- [39] Apos Neill P.F., Ben Azouz A., Vázquez M., *ET AL.*: 'Advances in three-dimensional rapid prototyping of microfluidic devices for biological applications', *Biomicrofluidics*, 2014, **8**, (5), p. 052112
- [40] Yuen P.K., DeRosa M.E.: 'Flexible microfluidic devices with three-dimensional interconnected microporous walls for gas and liquid applications', *Lab. Chip*, 2011, **11**, (19), pp. 3249–3255
- [41] Au A.K., Lai H., Utela B.R., *ET AL.*: 'Microvalves and micropumps for BioMEMS', *Micromachines*, 2011, **2**, (2), p. 179
- [42] Macedo Portela da Silva N., Letourneau J.-J., Espitalier F., *ET AL.*: 'Transparent and inexpensive microfluidic device for two-phase flow systems with high-pressure performance', *Chem. Eng. Technol.*, 2014, **37**, (11), pp. 1929–1937
- [43] Makamba H., Kim J.H., Lim K., *ET AL.*: 'Surface modification of poly (dimethylsiloxane) microchannels', *Electrophoresis*, 2003, **24**, (21), pp. 3607–3619
- [44] Toepke M.W., Beebe D.J.: 'PDMS absorption of small molecules and consequences in microfluidic applications', *Lab Chip*, 2006, **6**, (12), pp. 1484–1486
- [45] Kuddannaya S., Bao J., Zhang Y.: 'Enhanced in vitro biocompatibility of chemically modified poly(dimethylsiloxane) surfaces for stable adhesion and long-term investigation of brain cerebral cortex cells', *ACS Appl. Mater. Interfaces*, 2015, **7**, (45), pp. 25529–25538
- [46] Sivashankar S., Puttaswamy S.V., Tz-Shuian D., *ET AL.*: 'Emulated circulatory system integrated with lobule-mimetic liver to enhance the liver function', IEEE MEMS 2012, Paris, pp. 815–818